한국표면공학회지
Journal of the Korean Institute of Surface Engineering
Vol. 34, No. 5, Oct. 2001
<연구논문>

The electrochemical properties of PVD-grown WC-($Ti_{1-X}Al_X$)N multiplayer films in a 3.5% NaCl solution

S. H. Ahn, J.H. Yoo, J. G. Kim, H.Y. Lee, and J. G. Han

Center for Advanced Plasma Surface Technology (CAPST),
Sung Kyun Kwan University
300 Chunchun dong, Jangan-Gu, Suwon, 440-746, KOREA

Abstract

WC-($Ti_{1-X}Al_X$)N coatings of constant changing Al concentration were deposited on S45C substrates by high-ionization sputtered PVD method. The Al concentration could be controlled by using evaporation source for Al and fixing the evaporation rate of the metals (i.e, WC-$Ti_{0.86}Al_{0.14}N$, WC-$Ti_{0.72}Al_{0.28}N$, and WC-$Ti_{0.58}Al_{0.42}N$). The corrosion behavior of WC-($Ti_{1-X}Al_X$)N coatings in a deaerated 3.5% NaCl solution was investigated by electrochemical corrosion tests and surface analyses.

The measured galvanic corrosion currents between coating and substrate indicated that WC-$Ti_{0.72}Al_{0.28}N$ coating showed the best resistance of the coating tested. The results of potentiodynamic polarization tests showed that the WC-$Ti_{0.72}Al_{0.28}N$ coating deposited with 32W/㎠ of Al target revealed higher corrosion resistance. This indicated that the WC-$Ti_{0.72}Al_{0.28}N$ coating is effective in improving corrosion resistance. In EIS, the WC-$Ti_{0.72}Al_{0.28}N$ coating showed one time constant loop and increased a polarization resistance of coating (R_{coat}) relative to other samples.

Compositional variations of WC-($Ti_{1-X}Al_X$)N coatings were analyzed by EDS and XRD analysis was performed to evaluate the crystal structure and compounds formation behavior. Surface morphologies of the films were observed using SEM and AFM. Scratch test was performed to measure film adhesion strength.

1. INTRODUCTION

The interest in thin film technology has grown enormously during the last decades. Nitrides and carbides, mainly based on titanium, chromium and aluminum, have gained attention due to high hardness, chemical inertness, high wear resistance, and high corrosion resistance.

Using the cathodic arc deposition, we deposited superlattices of WC-($Ti_{1-X}Al_X$)N coatings. Superlattice coatings are nanometer-scale multilayers composed of two different alternating layers with a superlattice period, i.e. the bilayer thickness of two materials, ranging from 9 to 10nm, followed by its decrease for smaller periods due to interdiffusion and mixing at the interface[1]. A problem with cathodic arc vaporization source is that the arc causes the emission of molten globules that deposit on the film surface. Thus, these coatings often exhibit porosity and thus measurements of

the porosity are essential in order to estimate the corrosion resistance of a coated component.

The aim of this paper is to evaluate the corrosion protection of WC-$(Ti_{1-x}Al_x)N$ coatings. The corrosion characteristics of these materials were first investigated by a galvanic corrosion test, a potentiodynamic polarization test and next by electrochemical impedance spectroscopy (EIS) in a 3.5% NaCl solution at room temperature. Surface analysis techniques (XRD and EDS) were used to obtain information on the coated surface.

2. Experimental

2. 1 Material preparation and coating deposition

The chemical composition of the S45C substrate is listed in Table 1.

Table 1. Chemical composition of the S45C

Element	C	Si	Mn	P	S	Fe
wt. %	0.45	0.25	0.75	0.03	0.03	Bal.

Sampling 25×25mm was cut from the 5mm thick sheet, mechanically polished using 2000 grit SiC for the final step. For the deposition of WC-$(Ti_{1-x}Al_x)N$ coating, two Al arc cathodes were installed between Ti cathodes. A rotation substrate holder was used to obtain a layered structure, and the composition modulation wavelength of the superlattice was controlled by the rotation speed. Prior to coating, the substrate was subjected to high Ar ion etching. For the reduction of film stress[1], periodic layers (a bi-layer thickness : 20nm) of WC and $Ti_{1-x}Al_xN$ are deposited by selective arc discharge and modulating N_2 flow rate during the deposition of WC-$(Ti_{1-x}Al_x)N$ superlattice. The coating-substrate interface was modified by cathodic arc deposition of a TiN monolithic base layer (~10nm) between initiation of the WC-$(Ti_{1-x}Al_x)N$ superlattice coating deposition. The major deposition parameters used in this study are summarized in Table 2.

Table 2. WC-$Ti_{1-x}Al_xN$ PVD coating conditions

Plasma pre-cleaning	
Gas pressure	Ar 2.5×10^{-3} Torr
Bias voltage	-
Cleaning time	5 min
WC-$(Ti_{1-x}Al_x)N$ deposition	
Target power density	WC (3), Ti (3), Al (2) : 8targets WC : 50, Ti : 50, Al : 26, 32, 36 W/㎠
Base pressure	4×10^{-6} Torr
Working pressure	$1 \sim 1.5 \times 10^{-2}$ Torr
Bias voltage	- 600 V
Multi-arc condition	DC 50A
Temperature	150 ℃
Motor rotation	7 rpm
Coating thickness	2.1 ㎛

2. 2 Corrosion testing

A conventional three-electrode cell was used with the counter electrode and a saturated calomel electrode (SCE) as a reference electrode. All electrochemical experiments were performed under exclusion of oxygen in a 3.5% NaCl solution at room temperature. Potentiodynamic and EIS measurements have been obtained using an EG&G PAR 273A and EG&G Model 1025 frequency response detector with a computerized system for collection and analysis of the electrochemical data. Prior to the beginning of the polarization or EIS procedures, the specimens were kept in the solution for 1hr in order to establish the free corrosion potential (E_{corr}). Potentiodynamic polarization tests were obtained with a scan rate of 0.166mV/s from the initial potential of -250mV vs corrosion potential to the final potential of 400mV. The measurement of the EIS spectra was recorded in the 1mHz to 100kHz frequency range,

with a data density of five frequency points per decade. The applied AC signal amplitude was 10mV peak-to-peak and DC potential was set to corrosion potential. Long term data up to 168hr were taken at desired time intervals with the electrodes immersed in a 3.5% NaCl solution. The EIS results were analyzed with analysis software Z-view. A Gamry PC3/750 instrument connected a zero resistance ammeter (ZRA) was used for galvanic corrosion tests of the coated samples during 12hr.

2. 3 Adhesion and porosity measurement

To evaluate the adhesion of coatings, a specifically designed scratch tester was used to determine critical loads. The tests consisted of scratching the coated surface with stylus using predetermined loads, starting at 0 N and increasing to 100N. Each scratch had a length of 1㎝.

The degree of coating porosity has been determined quantatively by the through-coating porosity. By using electrochemical techniques, it is possible to estimate the porosity of these coatings. The porosity can be determined from the measured polarization resistance. The polarization resistance can be experimentally determined from dc polarization curve[2]. The porosity corresponds to the ratio of the polarization resistance of the un coated and the coated substrate[3].

$$P=\frac{Rp,u}{Rp,r-u}$$

where, P is the total coating porosity, $R_{p,u}$ is the polarization resistance of the substrate and $R_{p,r-u}$ is the measured polarization resistance of coatingsubstrate system.

2. 4 Surface analysis

The sample surface was observed using atomic force microscope (AFM). AFM analysis provided us the surface roughness as a function of the lateral length scale and an estimation of the columnar grain size and droplet distribution. The surfaces before- and after testing were examined in a scanning electron microscope (SEM).

3. Results and discussion

3. 1 Chemical composition and crystallography

The chemical compositions of the cathodic arc deposition coatings were obtained using an energy dispersive X-ray spectrometer (EDS). Fig. 1 shows the X-ray diffraction (XRD) pattern of the WC-($Ti_{1-x}Al_x$)N coatings. These data indicated that different phases and orientations dominate when the Al contents were varied. WC-($Ti_{1-x}Al_x$)N coating was identified to be a mixture of TiAlN ((111), (200)) and ß-WC_{1-x} (220), (311)) with a cubic B1 NaCl-type fcc structure and the lattice parameter was 0.417nm (TiN lattice = 0.426nm). Also, the above figures pointed out that the

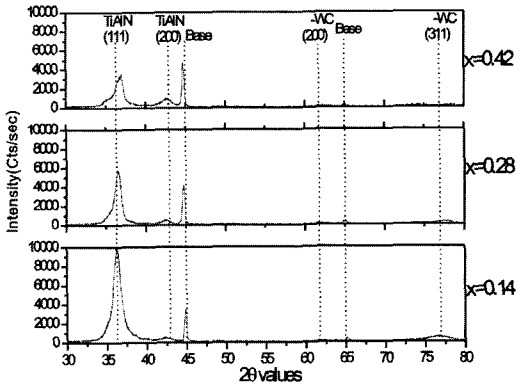

Fig. 1 XRD patterns for WC-($Ti_{1-x}Al_x$)N films with various Al contents

breadth of the diffraction peak increases with increasing Al content in the samples[4].

3. 2 Adhesion

Three scratch tests have been made and the averaged results are shown in Fig. 2. We consider the value of the critical load as the load at which the first adhesive failure mode occurs. The critical loads obtained are situated between 8.65 and 20.7N.

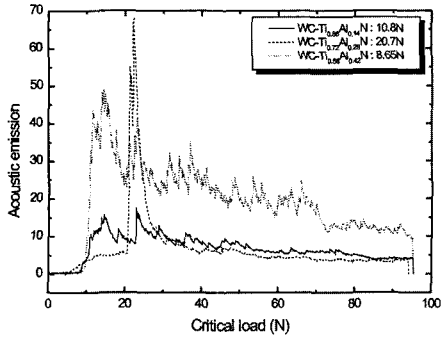

Fig. 2 Results of scratch adhesion tests for WC-$(Ti_{1-x}Al_x)N$ coatings

3. 3 Surface and cross-section structure

The morphologies of the coatings were investigated by AFM and SEM. In Fig. 3 and Fig. 4(a-c), the coatings contained not only circular droplets but also those with irregular shapes. Furthermore, it was found that the number of irregular droplets decreased when the Al target power density was 32W/㎠. The AFM micrograph (Fig. 4) shows that such pores can exist in regions close to macroparticle[5]. The droplets can form a local galvanic couple between one part as an anode and another as a cathode[6-9].

A typical SEM image (Fig. 4(f), the WC-$(Ti_{1-x}Al_x)N$ coatings after 168hr immersion) shows that

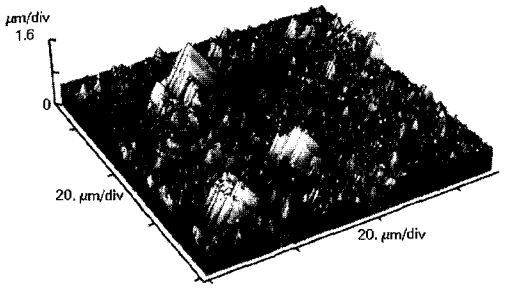

(a)

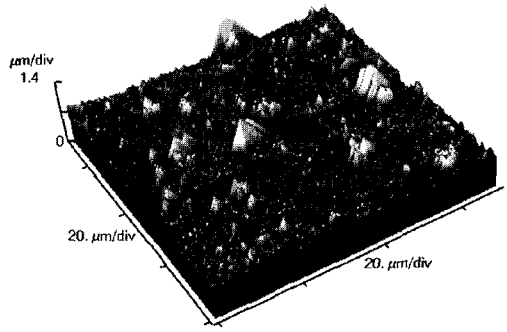

(b)

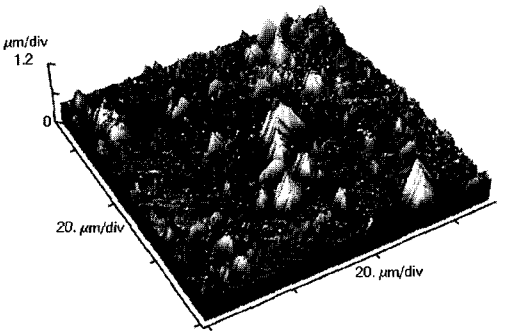

(c)

Fig. 3 Atomic force microscope of WC-$(Ti_{1-x}Al_x)N$ coatings (as-received).
((a) : $WC-Ti_{0.86}Al_{0.14}N$, (b) : $WC-Ti_{0.72}Al_{0.28}N$, (c) : $WC-Ti_{0.58}Al_{0.42}N$)

the coating is fragment. This cracking portion was probably dislodged by the hydrogen gas evolution ($2H_2O + 2e^- \Rightarrow H_2 + 2OH^-$) originating from within the pit.

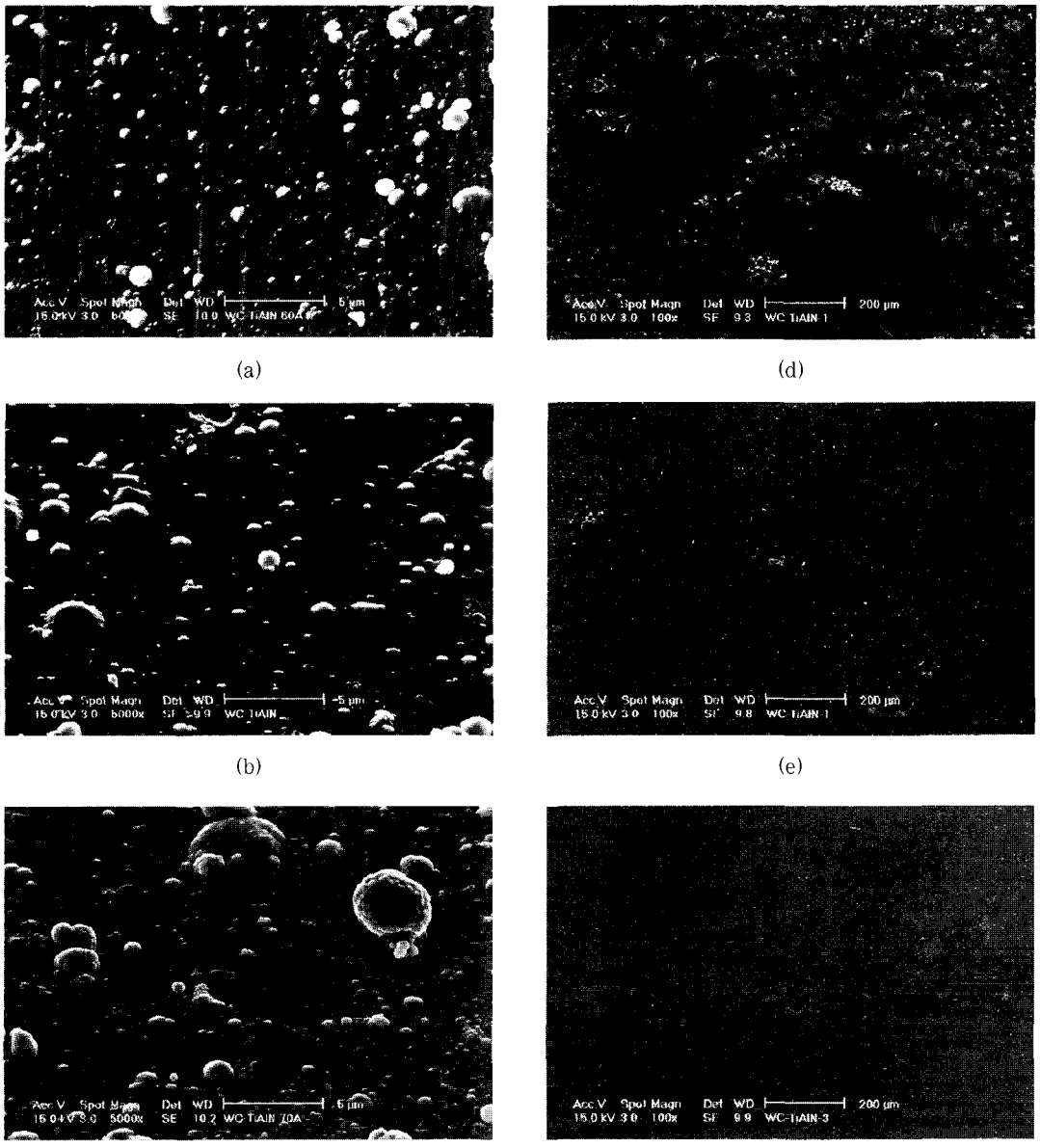

Fig. 4 SEM surface morphologies of WC-$(Ti_{1-x}Al_x)N$ superlattice coatings showing ; ((a) (d) : WC-$Ti_{0.86}Al_{0.14}N$, (b) (e) : WC-$Ti_{0.72}Al_{0.28}N$, (c) (f) : WC-$Ti_{0.58}Al_{0.42}N$; (a) (b) (c) : as-deposited coatings, (d) (e) (f) : after-tested coatings)

3. 4 Corrosion properties

Galvanic corrosion tests were accomplished using galvanic couple between the substrate and the coatings of WC-$(Ti_{1-x}Al_x)N$. It is observed that for all samples the galvanic corrosion current is small (Fig. 5). The measured corrosion currents indicate that WC-$Ti_{0.72}Al_{0.28}N$ coating show the best resistance of the coating tested. The current

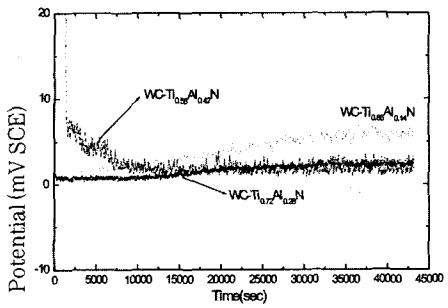

Current density (A/cm²)

Fig. 5 Results of galvanic corrosion tests for WC-$(Ti_{1-x}Al_x)N$ superlattice coatings

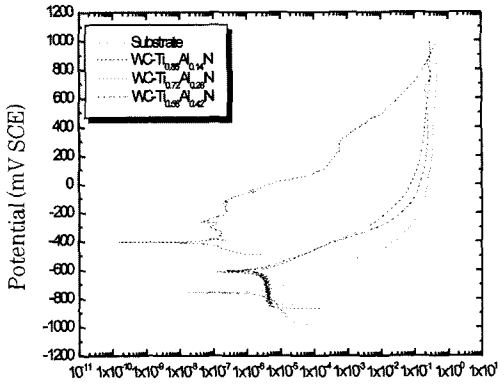

Current density (A/cm²)

Fig. 6 Polarization curves for WC-$(Ti_{1-x}Al_x)N$ in 3.5 %NaCl solution

of WC-$Ti_{0.86}Al_{0.14}N$ coating tended to increase during the test. WC-$Ti_{0.58}Al_{0.42}N$ coating showed a higher initial galvanic current density ($\sim 5\mu m/cm^2$) which was seen to decrease rapidly during the experiment.

The evolutions of the potentiodynamic polarization measurements of the WC-$(Ti_{1-x}Al_x)N$ coatings are shown in Fig. 6 and Table 3.

The anodic polarization curve of WC-$Ti_{0.72}Al_{0.28}N$ showed passive region and positioned in the left (noble) direction than others. The corrosion potential (-405.9mV) and corrosion density (169.6 nA/cm^2) of WC-$Ti_{0.72}Al_{0.28}N$ was nobler than others and displayed a passive behavior. It means that if the coating is porous, the coating is activated through the pores. Combining the equation of W. Tato et al[2]. with the electrochemical determinations gives a porosity rate of 0.109 for WC-$Ti_{0.86}Al_{0.14}N$, 0.09 for WC-$Ti_{0.72}Al_{0.28}N$, and of 0.111 for WC-$Ti_{0.58}Al_{0.42}N$ (Table 3). The porosity is somewhat higher in the WC-$Ti_{0.6}Al_{0.4}N$ coating than in the WC-$(Ti_{1-x}Al_x)N$ coated steels. The Al-rich coatings of WC-$(Ti_{1-x}Al_x)N$ coatings show a increased porosity and poor corrosion behavior. This was proved by H.A. Jehn[10]. and Jiang et al[11]. WC-$Ti_{0.72}Al_{0.28}N$ coating was declared as fully dense and low porosity[11]. In general, the corrosion current densities of the coated samples are low ($<6.875\mu A/cm^2$). The results of galvanic corrosion test and potentiodynamic polarization test were consistent with adhesion test and porosity measurement.

Fig. 7 shows the Bode plots for the WC-$(Ti_{1-x}Al_x)N$ coating applied directly to the substrate.

Table 3. Porosity of PVD coatings on S45C from DC polarization data

Samples	E_{corr} (mV)	i_{corr} ($\mu A/cm^2$)	R_p (ohm)	Calculated porosity
Substrate	-758.9	2.868	637	-
WC-$Ti_{0.86}Al_{0.14}N$	-581.5	0.0392	5823	0.109
WC-$Ti_{0.72}Al_{0.28}N$	-556.7	0.2034	7158	0.009
WC-$Ti_{0.58}Al_{0.42}N$	-558.2	0.5359	5759	0.111

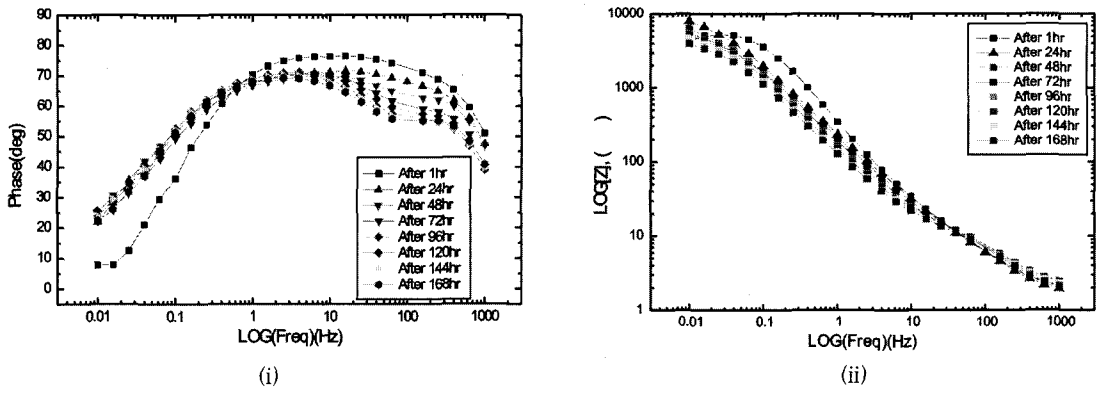

(i) (ii)

(a) WC-$Ti_{0.86}Al_{0.14}N$

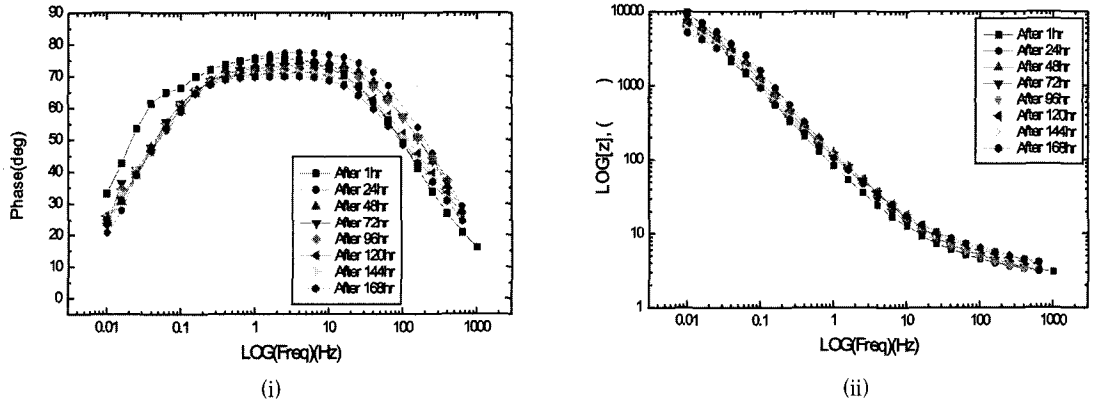

(i) (ii)

(b) WC-$Ti_{0.72}Al_{0.28}N$

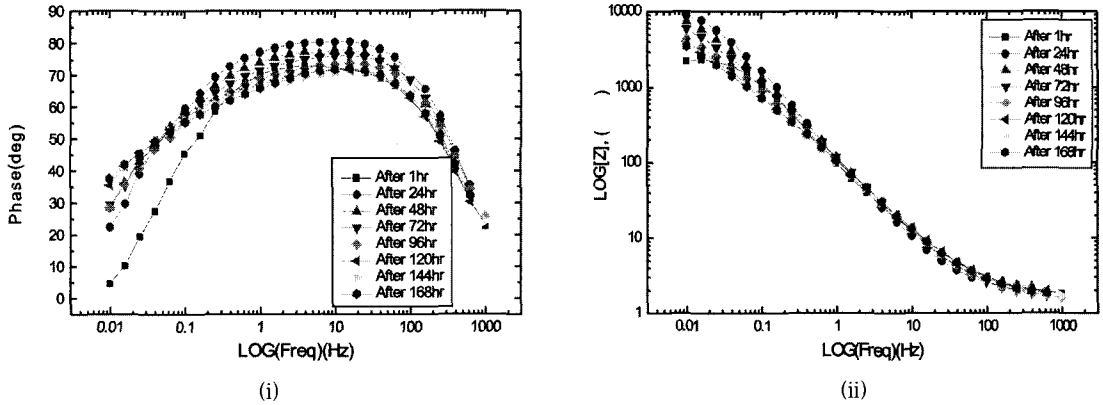

(i) (ii)

(c) WC-$Ti_{0.58}Al_{0.42}N$

Fig. 7 Bode plots for EIS data of WC-($Ti_{1-x}Al_x$)N in 3.5% NaCl solution for different exposure times ((i) : Phase(deg) vs LOG(Freq), (ii) LOG[Z] vs LOG[Freq])

The curves collected between 10mHz and 1kHz *after 1, 24, 48, 72, 96, 120, 144 and 168hr of testing* in a 3.5%NaCl electrolyte. The simulation fitting procedure was almost performed with the one-time constant coated-metal model, in shown Fig. 8 and the parameters presented in Table 4.

The equivalent circuit consists of the following elements: if two time constant, a solution resistance R_s of the test electrolyte between the working electrode and the reference electrode, a capacitance C_{pore} and a charge transfer R_{ct} for defects in the coatings, and a capacitance C_{coat} and a charge transfer resistance R_{pore} for the porosity resistance of coating layer.

In case of one time constant, the equivalent circuit is consisted of a capacitance C_{coat} and a charge transfer resistance R_{pore}.

During the fitting process, the capacitances were represented by a general diffusion which is defined as a constant phase element (CPE), which accounts for deviations from ideal dielectric behavior related to surface inhomogeneities. The factor n, defined as a CPE power, is an adjustable parameter that always lies between 0.5 and 1[12, 13]. The WC-$Ti_{0.86}Al_{0.14}N$ coating showed two-time constant behavior after 72hr immersion time. This result is caused by galvanic effect (Fig. 7) when the porous layer is exposured in the electrolyte.

The appearance of two time constant loops *after 72hr immersion time in the* WC-$Ti_{0.86}Al_{0.14}N$ coating indicated that the film had become defective and that corrosion was taking place under charge transfer control i.e, the WC-$Ti_{0.86}Al_{0.14}N$ coating is governed by the polarization resistance of charge transfer R_{ct}. The explanation for a

Table 4. Electrochemical parameters obtained by equivalent circuit simulation

Exposure Time/Al target Power density		R_s (Ωcm^2)	First time constant		R_{coat} (Ωcm^2)	Second time constant		R_{ct} (Ωcm^2)	WSS
			C_{coat} (Fcm^2)	n		C_{coat} (Fcm^2)	n		
1 hr	26 W/cm^2	1.596	1.942×10^{-4}	0.86	7191				0.01
	32	3.495	6.075×10^{-4}	0.89	8029				0.09
	36	1.571	7.176×10^{-4}	0.85	2788				0.01
24 hr	26 W/cm^2	1.175	3.601×10^{-4}	0.81	7966				0.25
	32	2.295	4.094×10^{-4}	0.88	8849				0.01
	36	1.032	3.737×10^{-4}	0.91	7573				0.01
72 hr	26 W/cm^2	1.343	4.485×10^{-4}	0.78	123	2.213×10^{-4}	1	6020	0.01
	32	2.942	5.531×10^{-4}	0.84	9449				0.01
	36	1.102	5.595×10^{-4}	0.86	4701				0.05
120 hr	26 W/cm^2	1.893	1.641×10^{-4}	0.91	21.26	3.687×10^{-4}	0.78	6008	0.01
	32	3.729	6.351×10^{-4}	0.82	9381				0.01
	36	1.443	8.084×10^{-4}	0.82	3236				0.09
168 hr	26 W/cm^2	1.571	1.850×10^{-4}	0.90	19.03	4.822×10^{-4}	0.78	4620	0.01
	32	4.038	7.207×10^{-4}	0.81	7433				0.03
	36	1.24	8.824×10^{-4}	0.82	2357				0.06

※ 26 W/cm^2 : WC-$Ti_{0.86}Al_{0.14}N$, 32 W/cm^2 : WC-$Ti_{0.72}Al_{0.28}N$, 36 W/cm^2 : WC-$Ti_{0.58}Al_{0.42}N$
WSS : Weighted sum of squares

charge transfer resistance R_{ct} comes from the penetration of the electrolyte through the pores or pinholes existing in the coating. This result matched with the porosity measurement. Also,

Fig. 7(c) shows a severe deviation of the phase angle in the low frequency region. Therefore, the penetration of electrolyte through the porous layer appeared to be greater than other coatings.

Fig. 7(b) shows two distinctive segments. The first, in the high frequency region, displays a linear increase of [Z] as frequency decreases. The second segment in the low frequency region exhibits a constant [Z] vs frequency. These results demonstrate that the corrosion resistance of WC-$Ti_{0.72}Al_{0.28}$ coating is high, i.e. since only small changes in the measured spectra occurred during the 168hr immersion test, this would suggest considerable electrochemical stability in a 3.5wt.% NaCl electrolyte[14]. Among these coatings, the coating resistance R_{ct} of WC-$Ti_{0.58}Al_{0.42}N$ coating was lower than other coatings.

From above results, WC-$Ti_{0.72}Al_{0.28}N$ coating would be the anticipitated best performance coating among the WC-$(Ti_{1-x}Al_x)N$ coating evaluated here.

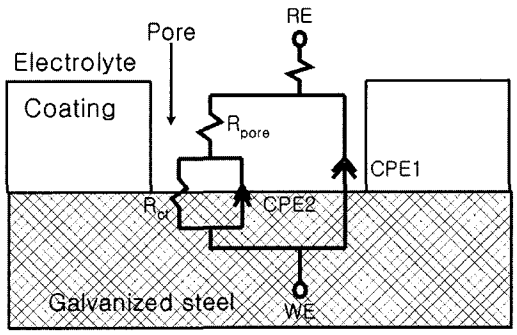

(RE:Reference Electrode, WE : Working Electrode)

(a)

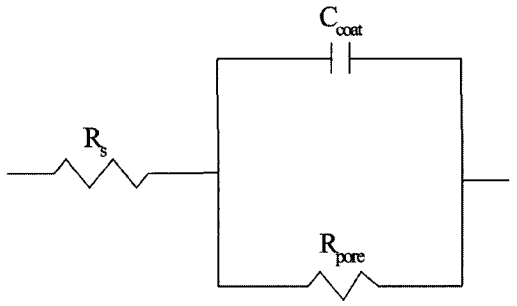

(b)

Fig. 8 The equivalent electronic circuit for a WC-$(Ti_{1-x}Al_x)N$ coating system.
(a) After 72hr immersion test of WC - $Ti_{0.86}Al_{0.14}N$, (b) All most coatings

4. Conclusions

1) A typical SEM image of WC-$Ti_{0.58}Al_{0.42}N$ coating shows that the coating is fragment. This cracking portion was probably dislodged by the hydrogen gas evolution.

2) WC-$Ti_{0.72}Al_{0.28}N$ coating represents better corrosion properties as indicated by the galvanic corrosion test. From the potentiodynamic polarization test, the polarization curve of WC - $Ti_{0.72}Al_{0.28}N$ showed passive region and positioned in the left (noble) direction than others. The corrosion potential of WC-$Ti_{0.72}Al_{0.28}N$ was nobler than others. All coated samples had much better corrosion resistance than the substrate.

3) From the EIS results, the Rcoat results obtained for these coatings all exhibited diminished values after 168hr exposure. Among these coatings, the coating resistance R_{ct} of WC-$Ti_{0.58}Al_{0.42}N$ coating was lower than other coatings. As the immersion time was prolonged WC-$Ti_{0.72}Al_{0.28}$ coating shows considerable electrochemical stability in a 3.5% NaCl electrolyte.

ACKNOWLEDGEMENT

The authors are grateful for the support provided by the Korea Science and Engineering Foundation through the Center for Advanced Plasma Surface Technology at SungKyunKwan University.

REFERENCES

1. Joo S. Yoon, Hyun S. Myung, Jeon G. Han, J. Musil, Surface and Coatings Technology 131 (2000) 372
2. B. Navinsek et al, Surface and Coatings T echnology 116-119 (1999) 476
3. W. Tato and D. Landalt, J. Electrochem. Soc., 1 45 (1998) 4173
4. T. Ikeda and H.Satoh, Thin Solid Films, 195 (1991) 99
5. H.W. Wang et al, Surface and Coatings Technology 135 (2000) 82-90
6. H.W. Wang et al, Surface and Coating Technology 126 (2000) 279
7. P. Marcus, J. Oudar, Corrosion Mechanisms in Theory and Practice, Marcel Dekker, Inc., 1995, 583
8. N. Voevodin et al, Surface and Coatings Technology 140 (2001) 29
9. D.A. Jones, Principles and Prevention of Corrosion, Macmillan Publishing Company, NewYork, (1991) 51
10. H.A. Jehn, Surface and Coatings Technology 125 (2000) 212
11. S.G. Jiang, D.L. Peng, X.Y. Zhao, L. Xie, Q. Li, Appl. Surf. Sci. 84 (1995) 373
12. Bary C. Syrett, Electrochemical Impedance and Noise, NACE, (1999) 45
13. J.Ross Macdonald, Impedance Spectroscopy, John Wiley & Sons, NewYork, (1987) 34
14. C.T. Chen, B.S. Skerry, Corrosion Science, 47 (1991) 598